

Dynamic Properties of Soft Clay and Loose Sand from Seismic Centrifuge Tests

M. H. T. Rayhani · M. H. El Naggar

Received: 20 August 2007 / Accepted: 13 March 2008
© Springer Science+Business Media B.V. 2008

Abstract Appropriate evaluation of shear modulus and damping characteristics of soils subjected to dynamic loading is key to accurate seismic response analysis and soil modeling programs. Dynamic centrifuge experiments were conducted at C-CORE (Memorial University of Newfoundland) centrifuge center to investigate the dynamic properties and seismic response of soft clay and dry loose sand strata. Soft clay with shear strength of about 30 kPa and well graded silica sand at about 35% relative density were employed in a rigid container to simulate local site effects. Several earthquake-like shaking events were applied to the model to evaluate variation of shear modulus and damping ratio with shear strain amplitude and confining pressure, and to assess their effects on site response. The estimated modulus reduction and damping ratio were compared to the predictions of empirical formulae and resonant column tests for both soft clay and loose sand. The evaluated shear modulus and damping ratio were found to be dependent on confining pressure in both soil types. Modulus variation in both soils agreed well with the empirical curves and resonant column test results. However, the sand

modulus values were slightly higher than the empirical relations and resonant column tests. This discrepancy is attributed to higher stress and densification of sand during large amplitude shaking applied to the model. The damping ratio at shear strains lower than 0.5% was in reasonable agreement with the empirical curves and the resonant column tests in both clay and sand models, but was generally higher at shear strain larger than 0.5%.

Keywords Centrifuge model · Loose sand · Soft clay · Shear modulus · Damping ratio

1 Introduction

Evaluation of dynamic soil properties is important for proper seismic response analysis and soil modeling programs. Numerical soil models use the variation of shear modulus and damping with strain level as basic input parameters for dynamic analyses. These parameters would ordinarily be based on element tests or on representative similar materials published in the literature.

Many researchers have used element tests such as cyclic triaxial or resonant column tests to derive shear modulus and damping parameters for various soil types. For example, Seed et al. (1986) and Rollins et al. (1998) evaluated gravel properties; Kokusho (1980) studied sand; and Hardin and Drnevich

M. H. T. Rayhani (✉) · M. H. El Naggar
Department of Civil & Environmental Engineering,
University of Western Ontario, London, ON,
Canada N6A 5B9
e-mail: mtofighr@uwo.ca; mrayhani@ce.queensu.ca

M. H. El Naggar
e-mail: helnaggar@eng.uwo.ca

(1972a) and Vucetic and Dobry (1991) evaluated clay properties. Field investigations have also been performed to study stiffness nonlinearity, based on earthquake motions (Chang et al. 1989; Zeghal et al. 1995). Such fieldwork can unfortunately only occur on the few instrumented sites.

Dynamic centrifuge testing represents an alternative technique for evaluation of soil behaviour (Brennan et al. 2005). Centrifuge testing avoids the limitations of soil type affecting the field testing, and the physical constraints of an element test. A few researchers have used the centrifuge data to estimate stiffness and damping parameters. Ellis et al. (1998) derived modulus and damping of very dense sand saturated with different pore fluids based on centrifuge testing. Elgamal et al. (2005) used centrifuge data to estimate stiffness, damping, and dilatancy characteristics of saturated dense Nevada sand.

In this paper, centrifuge accelerometer data were employed to identify both shear modulus and damping in clay and sand soils. The recorded time histories at different depths were used to back-calculate shear stress and shear strain response. The stress–strain data was then utilized to determine the shear modulus and damping ratio of both soft clay and loose sand. The estimated shear modulus and damping ratio were also compared with those from resonant column tests.

2 Centrifuge Tests

The centrifuge tests were conducted at 80-g on the 5.5-m diameter beam centrifuge at C-CORE, St.

Johns, NF, Canada. An electro-hydraulic earthquake simulator (EQS) was mounted on the centrifuge to apply a one dimensional prescribed base input motion. An equivalent shear beam model container (ESB) with inner dimensions of 0.73 m in length, 0.3 m in width, and 0.57 m in height was employed to simulate shear beam boundary conditions for the soil. At 80 g, the soil model simulated a prototype soil of 30 m in depth. The models were instrumented with extensive horizontal and vertical arrays of accelerometers and transformers (LVDT). Figure 1 shows the view of the soil models and instrumentation, with dimensions in prototype scale. Centrifuge tests on homogeneous soft clay and uniform loose dry sand are discussed here.

The artificial clay known as “glyben” (a mixture of sodium bentonite powder and glycerin) was used to simulate soft clay behaviour in these tests. The glycerin was added to bentonite to bring the glycerin content, GC, to about 45%. After mixing was completed, the mixture was covered with a plastic wrap and allowed to cure. This curing process produced a more even distribution of glycerin throughout the soil. Models were prepared by tamping of the split mould to obtain the desired void ratio (90% of maximum dry density). The homogeneity of each clay layer was checked by conducting vane shear tests. The soil properties are summarized in Table 1.

T-bar tests were performed to determine the continuous shear strength profile and were supplemented with vane shear tests, used as checks on the *T*-bar method. The undrained shear strength

Fig. 1 Centrifuge models configuration in prototype scale

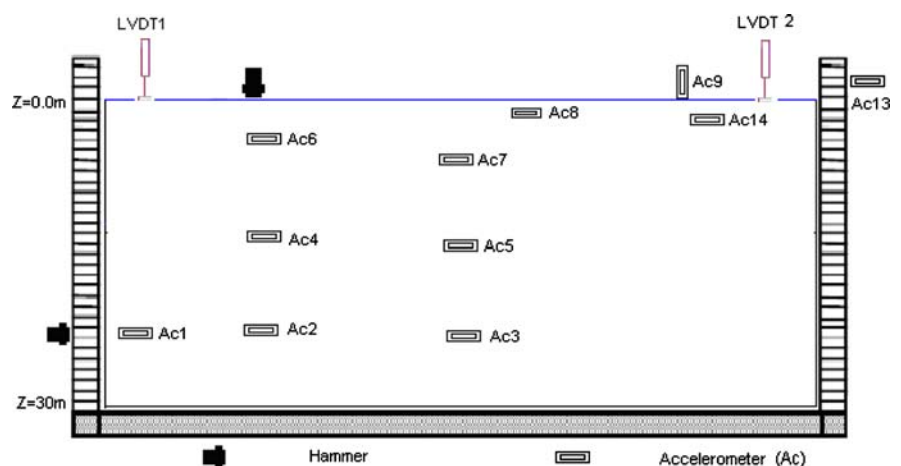


Table 1 Soil properties used in experimental tests

	Dry sand	Clay (Glyben)
Specification	A1 Standard sand	Bentonite + Glycerin
Pore fluid	None	Glycerin
Density (kg/m ³)	1,422	1,575
Void ratio (<i>e</i>)	0.90	1.23
Moisture content	Dry	45%
<i>D</i> ₅₀ (μm)	289	5
Average <i>V</i> _s (m/s)	149	73
Plasticity index	0	10.5

measured using the *T*-bar bearing resistance data varied between 40 and 60 kPa in soft clay (Rayhani and El Naggar 2008). The shear strength increased slightly with depth (i.e. with confining pressure). The vane shear result in model container was estimated about 35 kPa and 46 kPa before and after flight, respectively.

Figure 2 shows the settlement of clay model plotted versus log time. The vast majority of settlement occurred as the model swung up from 1 g to 80 g (the first 300 h prototype scale in Fig. 2). This initial (almost immediate) settlement is attributed to compaction of glyben. The remaining portion of the settlement is attributed to consolidation; however, the consolidation rate is very slow and the testing was completed under undrained conditions.

The sand soil used was well graded A1 white silica sand, medium angular with particle sizes in the range of 0.075–0.59 mm, *D*₅₀ = 0.288 mm, *e*_{min} = 0.637 and *e*_{max} = 1.046. Table 1 summarizes the material properties. At about 35% relative density (*D*_r), the sand was used to represent a loose soil formation with

prototype depth of 30 m. This loose model was prepared using a raining (pluviation) technique to provide a relatively uniform model with the desired relative density. The unit weight of the loose sand was 14.22 kN/m³.

Horizontal hammer blow tests were performed at depth 20 m to measure the shear wave velocity. The tests involved generating shear waves that could be detected by the arrays of accelerometers in the soil column. The test procedure consisted of striking the steel base plate of the model soil container with a sledge hammer. By identifying wave arrivals at each instrument, and knowing the instrument positions, differential travel times and shear wave velocities could then be computed. Table 2 shows shear wave velocities for each gravity level in both soil models. The average measured shear wave velocity was 73 m/s and 149 m/s for clay and sand, respectively.

Each model was subjected to 6 earthquake-like shaking events (Table 3). These events were imparted at centrifugal acceleration level of 80g. The input excitations were scaled versions of artificial west Canada earthquake (Seid-Karbasi 2003), and a scaled version of the Port Island ground motion recorded during the 1995 Kobe earthquake. Earthquake motions were applied using the electro-hydraulic simulator described by Coulter and Phillips (2003). Input motions varied between 0.07 g and 0.49 g.

3 Identification of Dynamic Soil Properties

Accelerometers were used to measure the soil acceleration at different depths (see Fig. 1): A2 and

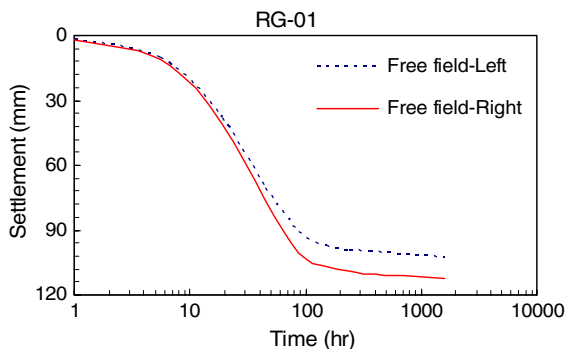


Fig. 2 Settlement curves of glyben soil from 1 g to 80 g in prototype scale

Table 2 Shear wave velocity of soil in centrifuge container

Gravity	Confining pressure (kPa)	Shear wave velocity (m/s)	
		Clay	Sand
10	35	50	125
20	70	55	131
30	106	65	139
40	142	70	143
50	177	80	156
60	213	85	161
70	248	90	167
80	283	92	172

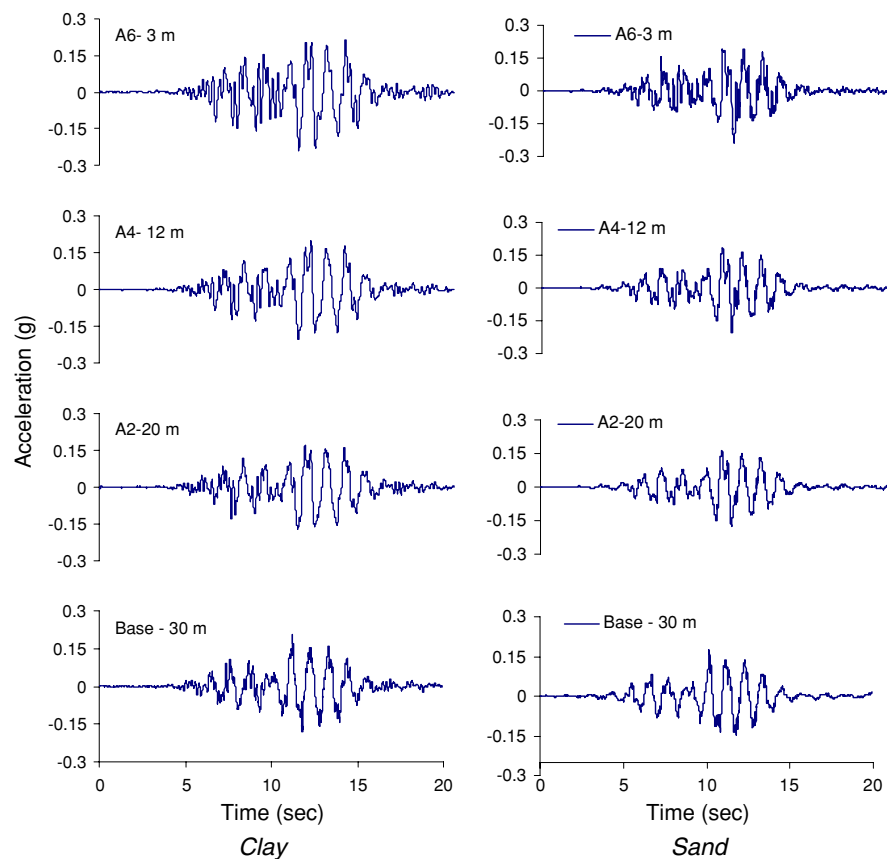
Table 3 Earthquake input motion in centrifuge tests

Event	Description	Prototype		Centrifuge (scale 1:80)	
		Peak acc. (g)	Frequency at peak (Hz)	Peak acc. (g)	Frequency at peak (Hz)
WCL	West Canada	0.1	0.93	8	75
WCM	West Canada	0.2	0.93	16	75
WCH	West Canada	0.39	0.93	31	75
KL	Kobe (1995)	0.07	2.19	5.5	175
KM	Kobe (1995)	0.22	2.19	17.6	175
KH	Kobe (1995)	0.49	2.19	39	175

A3 near the base; A4 and A5 at the middle of model; and A6 and A7 near the surface. Representative free field accelerations of a moderate event ($A_{max} = 0.2$ g) for both sand and clay soils are depicted in Fig. 3. Data from one weak event (WCL), one moderate event (WCM) and one strong shaking event (WCH) were used to calculate shear stress–strain histories and estimate dynamic soil properties in terms of shear modulus and damping ratio.

3.1 Evaluation of Shear Stress–Strain Histories

The shear stress and shear strain histories were evaluated using a one-dimensional shear beam idealization procedure proposed by Zeghal et al. (1995). Shear stress and shear strain response at a particular depth can be obtained using the recorded lateral accelerations, assuming 1D vertically propagating shear waves.

Fig. 3 Representative acceleration during WCM event in clay and sand

Shear stress at any depth was estimated by integrating the equation of motion at any depth as:

$$\tau(z, t) = \int_0^z \rho \ddot{u} dz \quad (1)$$

where z is depth coordinate; τ is horizontal shear stress; \ddot{u} is horizontal acceleration and ρ is density (Zeghal et al. 1995).

For shear strain calculation, displacement records were first obtained through double integration of the corresponding recorded acceleration histories. The shear strain histories were then evaluated using the displacement data and the spacing between accelerometers.

Accuracy of shear stress and strain estimates is a function of accelerometer configuration, data processing and employed analysis technique (Zeghal et al. 1995). Displacement histories from integration of accelerations often include base line drifts. Band pass filters were employed between 0.03 Hz and 25 Hz to eliminate noise at high frequency and drifts at low frequency range. The filter bandwidths were selected wide enough to preserve the real shear stress and strain characteristics of the soil model. Considering the close spacing of accelerometers and simplicity of analysis, first order linear interpolation between accelerations and second order interpolation between displacements were employed to evaluate the shear stress and strain, respectively.

The estimated seismic shear stress and shear strain histories are related by the soil shear stiffness characteristics at each accelerometer level (Zeghal et al. 1995). The shear stress–strain hysteresis are shown in Fig. 4 at depths 3 m, 12 m, and 20 m during WCM shaking event for the clay model. The shear stress–strain hysteresis at different depths in the sand model during different shaking events is shown in Fig. 5. The hysteresis loop slope, and thus the soil shear stiffness, decreased with strain amplitude as it propagated from the base to the surface.

Shear stress–strain hysteresis during low amplitude earthquake (WCL) provided low strain soil response. The shear strain level increased with applying stronger shaking events to the soil model (WCM and WCH). The hysteresis loop slope increased with the depth of accelerometer, indicating the effect of confining pressure on soil shear stiffness. The shear stress–strain area, and thus the soil

damping, increased with strain amplitude and decreased with increase of depth. These behaviors are in good agreement with soil behavior observed from element tests and reported results in the literature.

3.2 Calculation of Shear Modulus and Damping Ratio

The soil shear modulus and equivalent damping ratio were evaluated from the stress–strain cycles of the WCL, WCM, and WCH earthquake shakings at different depths as a function of shear strain amplitude. These shaking events provided dynamic soil properties at different confinement levels, with shear strain ranging from about 0.1 to 1.0%. The procedure for estimating these properties is shown in Fig. 6 (Kramer 1996). Shear modulus in clay and sand models was estimated using the secant slope of the representative shear stress–strain loop for each shaking event at 3 m, 12 m, and 20 m depth.

In order to compare measured shear moduli with standard degradation curves, a value for the small-strain shear modulus (G_{\max}) is required. The G_{\max} was calculated from the shear wave velocity measured using the hammer test, i.e.

$$G_{\max} = \rho v_s^2 \quad (2)$$

where V_s is shear wave velocity and ρ is soil density. Table 4 shows G_{\max} values at different depths for both clay and sand soils. These values were used to normalize the shear moduli and depict the degradation curves.

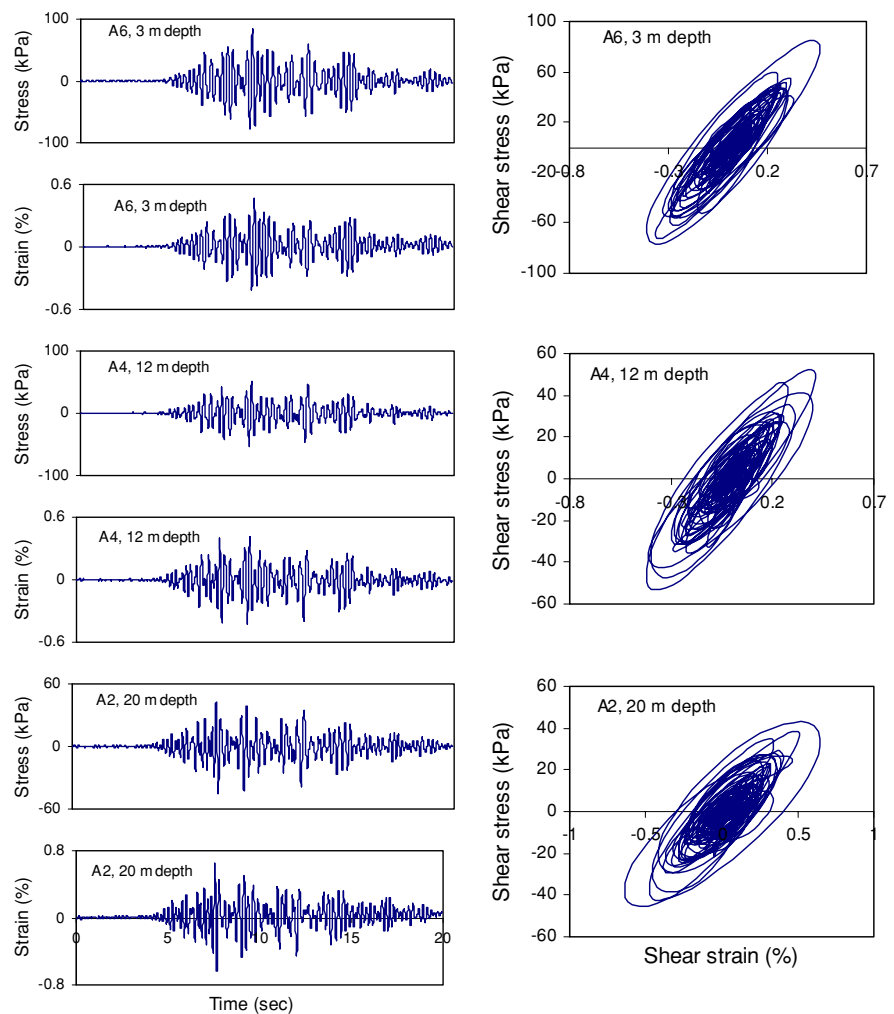
The damping ratio was calculated from selected stress–strain loops at 3 m, 18 m, and 27 m using the area of the actual shear stress–strain loop (Fig. 5), i.e.:

$$\xi = \frac{A_{\text{loop}}}{2\pi G \gamma^2} \quad (3)$$

where ξ is damping ratio, A_{loop} is the area of the stress–strain loop, G is shear modulus, and γ is shear strain.

Three stress–strain cycles were sampled individually from each series of shear stress–strain loops, and used to estimate the shear modulus and damping ratio as a function of shear strain. Thus, three shear modulus and damping values were evaluated for each event at each depth.

Fig. 4 Shear stress–strain histories at different depths during WCM event in clay



4 Assessment of Shear Modulus

The shear modulus values from centrifuge tests were normalized by the G_{\max} to obtain the shear modulus degradation curves for both soft clay and loose sand. The curves were compared with standard formula and resonant column tests.

4.1 Soft Clay

Three accelerometers at different depths were used to estimate the shear modulus at different values of confining pressure. The accelerations were increased from weak to strong earthquakes to obtain the shear modulus at different strain levels. The shear modulus was then normalized by G_{\max} (Table 4).

The data are plotted in Fig. 7 against the design curves of Hardin and Drnevich (1972b), Vucetic and Dobry (1991) and Kokusho et al. (1982). A best fit curve through appropriate data (confinement, 300 kPa) from resonant column tests on glyben clay (Rayhani and El Naggat 2008) is also included and compared with centrifuge data.

The estimated experimental data in Fig. 7 displays the trend and values that would be expected throughout the strain range tested. The centrifuge data are in good agreement with the corresponding empirical relationships. The shear modulus at all shear strain levels is remarkably close to the resonant column results and relationship proposed by Kokusho et al. (1982) for clay, while these data are noticeably higher than the design curves suggested by Hardin and

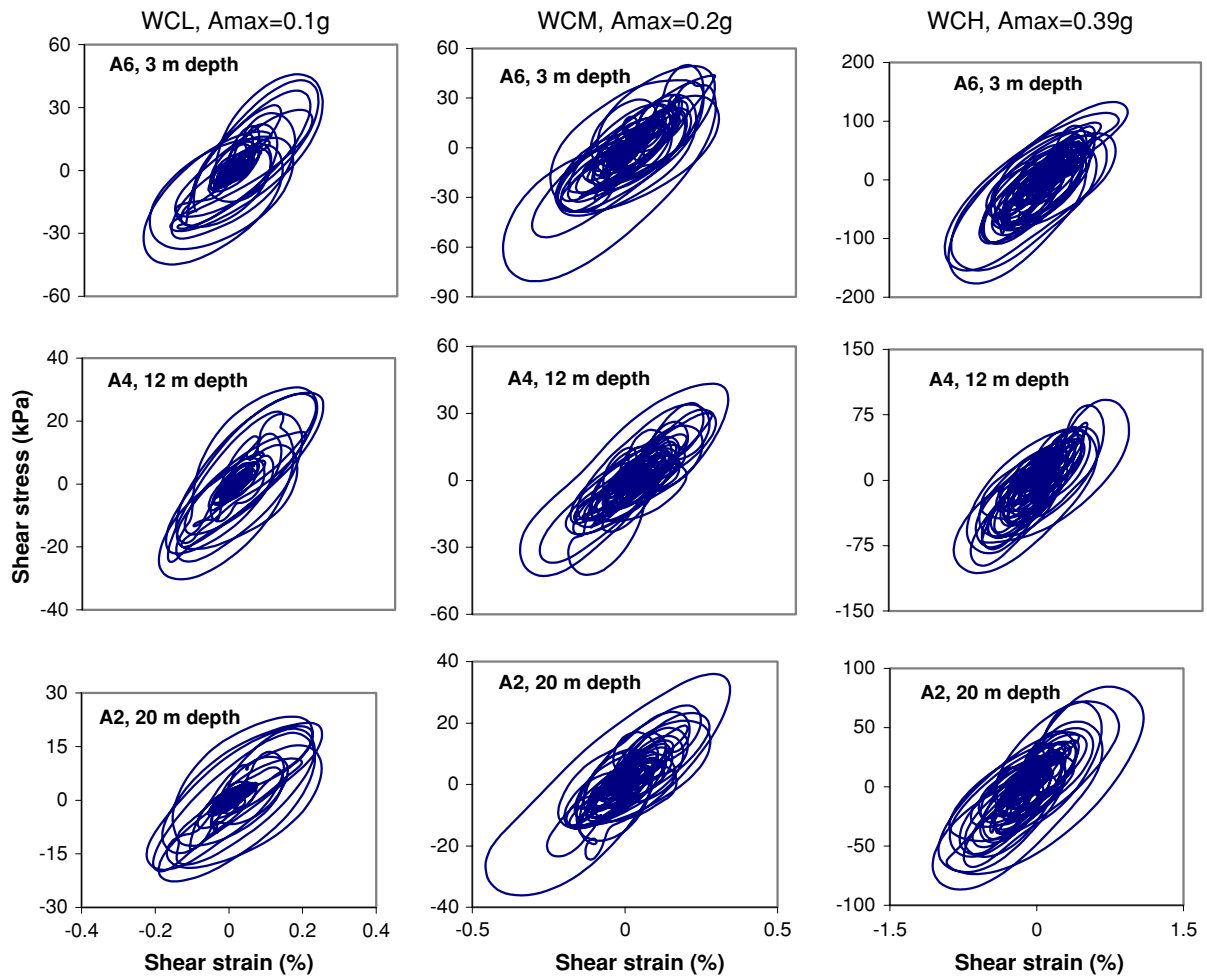


Fig. 5 Shear stress–strain histories at different depths during all shaking events in sand

Drnevich (1972b), and Vucetic and Dobry (1991). The shear modulus ratio (G/G_{\max}) decreased with the shear strain amplitude and increased with depth, indicating increase with confining pressure.

4.2 Dry Sand

Shear modulus values were derived from 3 accelerometers aligned vertically up the free field model. These values were normalized by the G_{\max} derived from the shear wave velocity measured using the hammer test. The shear modulus degradation curves for accelerometers A6 (3 m depth), A4 (12 m depth), and A2 (20 m depth) are shown in Fig. 8, and are compared with the curves generated from the empirical relationships given by Hardin and Drnevich (1972b) and Seed and Idriss (1970) for dry fine sands.

A best fit through results obtained from appropriate resonant column data (at 300 kPa confining pressure) is also plotted in Fig. 8 for comparison.

As it can be seen from Fig. 8, estimated damping values are close to the resonant column results and the empirical relations proposed by Hardin and Drnevich and upper band of Seed–Idriss (1970) at all strain levels, especially in lower depths. However, most of the centrifuge data is seen to be higher than that dictated by the empirical relations and element test results. This behaviour might be attributed to densification of loose sand during higher magnitude events (WCH). The relative density of loose sand increased by about 5% after the WCH shaking event. Figure 8 also shows that the shear modulus increased with increasing confining pressure (or depth) in all strain range.

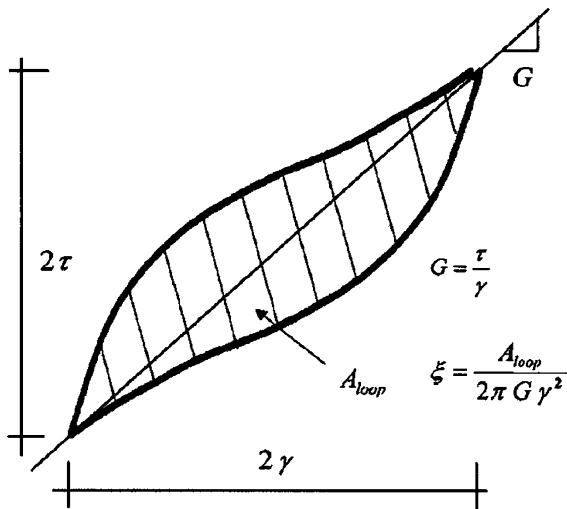


Fig. 6 Evaluation of shear modulus and damping from stress–strain loop (Kramer 1996)

Table 4 G_{max} values at different depths for clay and sand

Model depth (m)	Clay		Sand	
	Confinement (kPa)	G_{max} (MPa)	Confinement (kPa)	G_{max} (MPa)
3	47	8.7	42	34
12	189	10.8	170	42
20	315	13.3	284	45

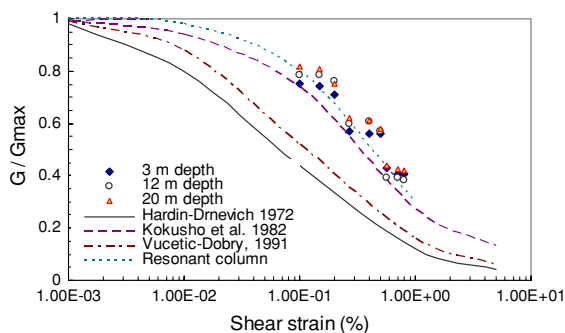


Fig. 7 Shear modulus degradation of glyben clay

5 Assessment of Damping Ratio

The damping ratios values were estimated from selected shear stress–strain loop as a function of shear strain during centrifuge model earthquakes. These data were compared with the design damping degradation curves and those obtained from resonant column tests.

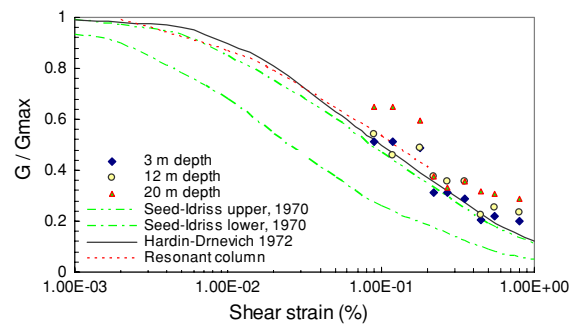


Fig. 8 Shear modulus degradation of dry sand

5.1 Soft Clay

The damping ratios obtained for the glyben soil are shown in Fig. 9. The damping data from the resonant column tests and standard design curves of Hardin and Drnevich (1972b), Vucetic and Dobry (1991) and Kokusho et al. (1982) are also shown to compare the centrifuge shear modulus. Figure 9 shows that the damping ratio decreased with the increase in depth (or confining pressure), and increased with shear strain amplitude. These behaviors are in agreement with the resonant column results and appear in all empirical curves.

In general, damping ratios seem to increase with shear strain amplitude, and decrease with depth. The estimated centrifuge damping ratio at all shear strain levels appears to fall along the empirical relations of Hardin and Drnevich (1972a) and the resonant column results. However, the damping ratio data is slightly higher than the corresponding Hardin and Drnevich empirical curves, at shear strain larger than 0.5%. Such scatter in estimated damping values were also reported by Zeghal et al. (1995) and Brennan et al.

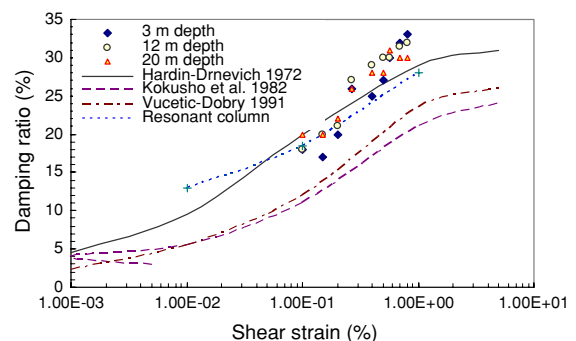


Fig. 9 Identified damping and empirical relationships for glyben clay

(2005). The centrifuge data are noticeably far from the design curves suggested by Kokusho et al. (1982) and Vucetic and Dobry (1991) for fine grained soils.

5.2 Dry Sand

Figure 10 presents the damping ratios obtained from the centrifuge tests together with a best fit of the damping ratio of the resonant column tests. The damping ratio curves generated from the equations of Hardin and Drnevich (1972b) and Seed and Idriss (1970) are also included in Fig. 10.

As it would be expected, the centrifuge damping ratios show confinement dependence, in agreement with previous studies. The damping ratio decreased with depth (or confining pressure), and increased with shear strain amplitude. The comparison of the centrifuge data with empirical relations and element tests shows a reasonable agreement with the empirical curves, especially the relation proposed by Hardin and Drnevich (1972a) and Seed and Idriss (1970). The damping ratio at low strain levels is close to that obtained from resonant column tests. However, the damping ratio at shear strain magnitude larger than 0.5% is slightly higher than the corresponding Hardin and Drnevich (1972a), Seed and Idriss (1970) empirical curves. This scatter in damping could be due to densification of loose sand and stronger soil particle contact during strong earthquake excitation. Frictional energy loss in the soil skeleton is increased as the soil particles gain contact with each other (Brennan et al. 2005; Zeghal et al. 1995). Such scatter in damping was also observed in investigation of damping such as Brennan et al. (2005). The damping ratio is in reasonable agreement

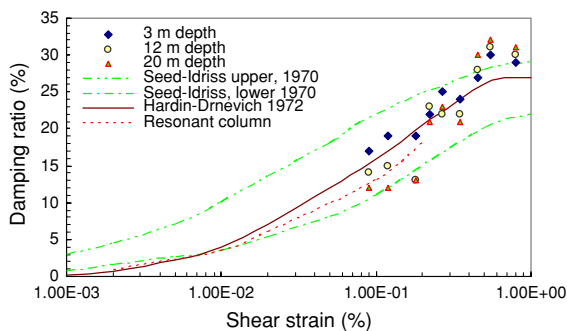


Fig. 10 Calculated damping and empirical relationships for dry sand

with the empirical curves of Hardin and Drnevich, and Seed and Idriss and the resonant column results for shear strains smaller than 0.5%.

6 Summary and Conclusions

Centrifuge testing of ground response for both soft clay and dry loose sand models were used to produce acceleration data at different shear strain and confinements. Shear stress–strain hystereses were calculated from the acceleration data, assuming one-dimensional shear beam behaviour. Shear modulus and damping ratio for both soft clay and loose dry sand were estimated from the stress–strain hysteresis. Shear modulus data were normalized by G_{\max} to obtain degradation curves and study their variation in a range of strain levels. The estimated centrifuge data were compared with those from resonant column tests and standard design curves to evaluate the computed data for both soft clay and loose sand.

In general, the centrifuge test results were in reasonable agreement with the empirical trends, and lead to an improved confidence in the proposed curves at weak levels of shaking where data is rare. The evaluated shear modulus and damping ratio showed reasonable confinement dependence in both models. Shear modulus data increased with depth in both clay and sand, while damping ratio decreased as the accelerometer depth increased.

The identified centrifuge modulus reduction seemed to be relatively close to the empirical relations and the element test results, in comparison with other published data in the literature. However, in dry sand the modulus values were slightly higher than the empirical relations, which could be attributed to densification of loose sand during earthquake excitations.

The damping characteristics at shear strain smaller than 0.5% is in reasonable match with the empirical curves and the resonant column tests in both clay and sand models. However there is a scatter in the data at shear strain larger than 0.5% in both soils. In case of dry sand, it could be due to stronger soil particle contact and frictional energy loss in the soil skeleton.

Acknowledgements The authors would like to thank Dr. Ryan Phillips Director of C-CORE for his guidance and support during the centrifuge testing phase of this research and Gerry, Susan, Karl, Don Cameron, and Derry for their assistance in the centrifuge tests. Their help is gratefully acknowledged.

References

- Brennan AJ, Thusyanthan NI, Madabhushi SPJ (2005) Evaluation of shear modulus and damping in dynamic centrifuge tests. *J Geotech Geoenviron Eng ASCE* 131(12):1488–1497
- Chang C-Y, Power MS, Tang YK, Mok CM (1989) Evidence of nonlinear soil response during a moderate earthquake. In: *Proceedings of the 12th international conference on soil mechanics and foundation engineering*, Balkema, Rotterdam, The Netherlands, pp 1927–1930
- Coulter SE, Phillips R (2003) Simulating submarine slope instability initiation using centrifuge model testing. Paper ISSMM-062 1st International symposium on submarine mass movements and their consequences, EGS-AGU-EUG Joint Assembly Meeting, Nice. Kluwer Academic Publishers, Netherlands
- Elgamal A, Yang Z, Lai T, Kutter B, Wilson DW (2005) Dynamic response of saturated dense sand in laminated centrifuge container. *J Geotech Geoenviron Eng ASCE* 131(5):598–609
- Ellis EA, Soga K, Bransby MF, Sata M (1998) Effect of pore fluid viscosity on the cyclic behaviour of sands. In: *Proceedings of the centrifuge 98*, Tokyo, Japan. A.A. Balkema Publishers, pp 217–222
- Hardin BO, Drnevich VP (1972a) Shear modulus and damping in soil: measurement and parameter effects. *J Soil Mech Found Eng Div ASCE* 98(6):603–624
- Hardin BO, Drnevich VP (1972b) Shear modulus and damping in soil: design equations and curves. *J Soil Mech Found Eng Div ASCE* 98(7):667–692
- Kokusho T (1980) Cyclic triaxial test of dynamic soil properties for wide strain range. *Soils Found* 20(2):45–60
- Kokusho T, Yoshida Y, Esashi Y (1982) Dynamic properties of soft clay for wide strain range. *Soils Found* 22(4):1–18
- Kramer SL (1996) *Geotechnical earthquake engineering*. Prentice Hall, Upper Saddle River, NJ
- Rayhani MHT, El Naggar MH (2008) Characterization of glyben for seismic application. *Geotech Test J ASTM* 31(1), paper ID: GTJ100552
- Rollins KM, Evans MD, Diehl NB, Daily WD (1998) Shear modulus and damping relationships for gravels. *J Geotech Geoenviron Eng ASCE* 124(5):396–405
- Seed HB, Idriss IM (1970) Soil moduli and damping factors for dynamic response analyses. Rep. No. EERC-70/10, Earthquake Engineering Research Center, Univ. of California at Berkeley, Berkeley, CA
- Seed HB, Wong RT, Idriss IM, Tokimatsu K (1986) Moduli and damping factors for dynamic analyses of cohesionless soils. *J Geotech Eng ASCE* 112(11):1016–1032
- Seid-Karbasi M (2003) Input motion time histories for dynamic testing in the c-core centrifuge facilities. Report No. 2003/01, University of British Columbia
- Vucetic M, Dobry R (1991) Effect of soil plasticity on cyclic response. *J Geotech Eng ASCE* 117(1):89–107
- Zeghal M, Elgamal A-W, Tang HT, Stepp JC (1995) Lotung downhole array. II: evaluation of soil nonlinear properties. *J Geotech Eng* 121(4):363–378